STATE OF THE CLIMATE IN 2016

Special Supplement to the
Bulletin of the American Meteorological Society
Vol. 98, No. 8, August 2017

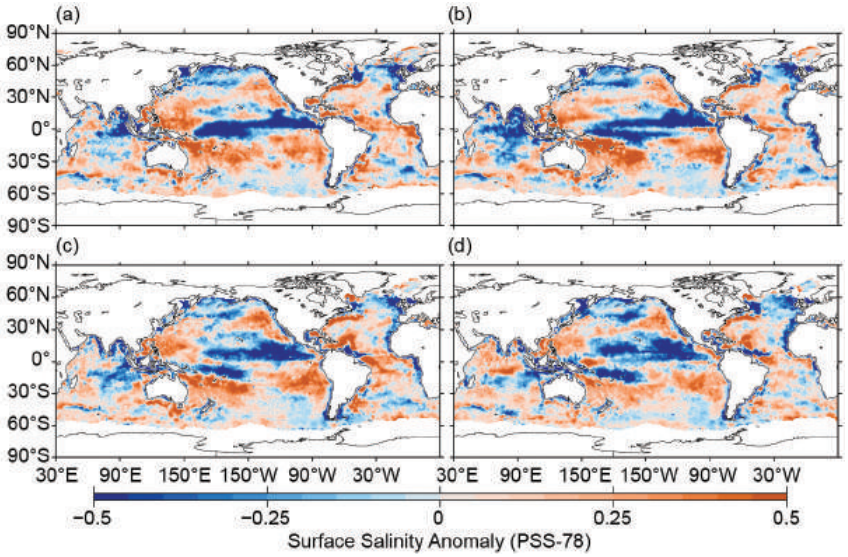

Fig. 3.8. Seasonal maps of SSS anomalies (colors) from monthly blended maps of satellite and in situ salinity data (BASS; Xie et al. 2014) relative to monthly climatological 1955–2012 salinity fields from WOA13v2 for (a) Dec–Feb 2015/16, (b) Mar–May 2016, (c) Jun–Aug 2016, and (d) Sep–Nov 2016. Areas with maximum monthly errors exceeding 10 PSS-78 are left white.

region, fresh anomalies moved poleward over the course of the year, likely reflecting both advection of anomalously fresh waters that built up around the equator owing to strong precipitation and the eastward migration of the western Pacific fresh pool during the 2015/16 El Niño, and subsequent upwelling of saltier water along the equator and reductions of precipitation in the eastern equatorial Pacific with the transition to weak La Niña conditions by the end of 2016.

Sea surface salinity trends for 2005–16 exhibit large-scale patterns in all three oceans (Fig. 3.7c). These trends are estimated by local linear fits to annual average SSS maps from Argo data with a starting year of 2005, because that is when Argo coverage became near-global. There are regions of increasing salinity near the subtropical salinity maxima in each basin, except in the eastern subtropical North Atlantic. In the Pacific, this increasing salinity trend is at lower latitudes in the west than in the east. In contrast, there are regions in the Southern Ocean and the subpolar North Atlantic and North Pacific where the trend is toward freshening. Again, these patterns are reminiscent of the multidecadal changes discussed above and suggest a discernible intensification of the hydrological cycle over the ocean over the last dozen years. However, the freshening trend in much of the subpolar North Atlantic is roughly coincident with a trend toward low upper ocean heat content (see Fig. 3.4c), suggesting an eastward expansion of the subpolar gyre that may be linked to reductions in the AMOC over the past decade (Section 3h). In addition, the freshening trend in the eastern Indian Ocean is likely owing to a lingering signature of the strong 2010–12 La Niña, refreshed by anomalously strong precipitation in 2016 (see Fig. 3.12). Freshening trends in the eastern tropical Pacific are likely owing to interannual ENSO variability and not necessarily reflective of a long-term trend. The region to the northwest of the Gulf Stream and in the Gulf of Mexico is trending strongly saltier, as well as warmer (Section 3c).

3) Subsurface salinity—J. Reagan, T. Boyer, C. Schmid, and R. Locarnini

The 2016 Atlantic Ocean basin-average monthly salinity anomaly pattern (Fig. 3.9a) is similar to the previous decade, with large (>0.05) salty anomalies in the upper 200 m decreasing with depth to little/no change near 700 m and very weak (±0.005) anomalies between 700 and

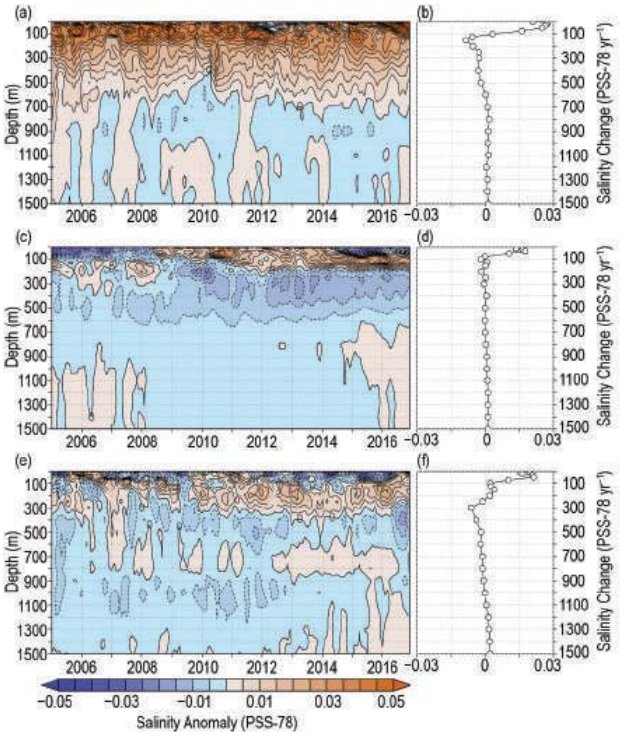

Fig. 3.9. Average monthly ocean salinity anomalies from 0–1500 m for the (a) Atlantic from 2005–16 and (b) the change from 2015 to 2016; (c) Pacific from 2005–16 and (d) the change from 2015 to 2016; and (e) Indian from 2005–2016 and (f) the change from 2015 to 2016. Data were smoothed using a 3-month running mean. Anomalies are relative to the long-term WOA13v2 monthly salinity climatology (Zweng et al. 2013).

1500 m. From 2015 to 2016, salinity increased in the upper 100 m with a maximum increase of ~0.03 near the surface (Fig. 3.9b). From 125 to 600 m, 2016 was slightly fresher than 2015 with a maximum decrease of ~ −0.01 at 150 m.

The upper 30 m of the Pacific Ocean has been fresh since mid-2014, with the exception of weak (±0.005) anomalies in early 2016 (Fig. 3.9c). This pattern contrasts with positive near-surface salinity anomalies from mid-2008 through mid-2014 (Fig. 3.9c). Salty anomalies from 100 to 200 m have been persistent since mid-2011, as have fresh anomalies (< −0.005) from 200 to 500 m since 2009. From 2015 to 2016, salinity increased in the upper 75 m, approaching ~0.02 at 30 m (Fig. 3.9d), in stark contrast to the freshening that was seen between 2014 and 2015 (Reagan et al.

SIDEBAR 3.2: DEEP ARGO: SAMPLING THE TOTAL OCEAN VOLUME—N. ZILBERMAN

Full-depth ocean temperature–salinity profiling is essential for closing global and regional budgets of heat, freshwater, and steric sea level; for quantifying the processes causing sea level change; for accurately estimating the meridional overturning circulations; and for assimilating global ocean reanalyses and initializing ocean forecast systems. Deep-ocean temperature and salinity observations have been limited to sparse shipboard hydrographic sections repeated approximately every decade and even sparser deep ocean moorings. The need for more frequent sampling of the full ocean volume has long been recognized by the scientific community but has not, until recently, become practical.

Measuring the variability of temperature and salinity in the deep ocean is technically challenging. Deep-ocean properties show significant large-scale trends on decadal time scales in some deep basins, with the strongest anomalies at high latitudes near water mass formation regions (Purkey and Johnson 2010, 2013; Desbruyères et al. 2016). The Argo Program's international partnership proposes to meet the technical challenge by deploying a new generation of Deep Argo floats globally. At present, Argo operates a total of nearly 4000 floats, homogeneously distributed over the global ocean, measuring temperature and salinity profiles to 2000-m depth. Deep Argo will extend conventional Argo sampling to the ocean bottom.

A Deep Argo workshop held in May 2015 articulated key scientific issues, initiated implementation planning for a global Deep Argo array, and identified broad-scale requirements for Deep Argo float measurement of temperature, salinity, and ocean circulation (Zilberman and Maze 2015). Deep Argo will consist of about 1200 floats distributed globally at 5° latitude × 5° longitude spacing. Deep Argo floats will sample the water column from the sea surface to 4000 or 6000 m, depending on the float model used, every 15 days. Statistical analysis indicates that such an array will significantly reduce uncertainties in the global decadal trends in ocean heat content and the steric contribution to sea level rise (Johnson et al. 2015b). The standard error of the trend in global ocean heat content for the 2000–6000 m depth range will decrease to ±3 TW (1 TW = 10^{12} W) using Deep Argo data, down from ±17 TW

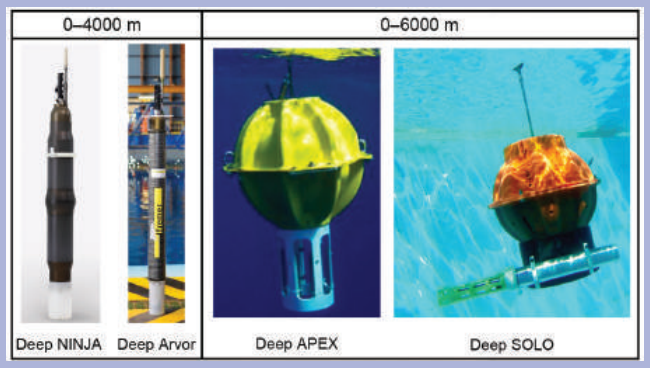

Fig. SB3.2. Deep Argo float models: Deep NINJA, Deep Arvor, Deep APEX, and Deep SOLO.

based on repeat hydrographic transects. With 15-day cycling, the deep Argo array will have a refresh time, based on float battery energy capacity and consumption, of five years, similar to the 0–2000 m Argo array.

The implementation of a sustainable Deep Argo array will not rely on a single float design. Technology advances have provided pressure housings, pumping systems, and other float components capable of operation at abyssal pressures. Four Deep Argo float models have been developed (Fig. SB3.2), including the 6000-m Deep SOLO (U.S.) and Deep APEX (U.S.) floats, and the 4000-m Deep Arvor (France) and Deep NINJA (Japan) floats. Comparisons of these Deep Argo float models are ongoing to assess their performance, robustness, and cost-effectiveness. Conductivity–temperature–depth (CTD) sensors mounted on Deep Argo floats include an extended-depth version of the SeaBird Electronics SBE-41 on Deep Arvor and Deep NINJA, and the new SBE-61 on Deep SOLO and Deep APEX. Initial results from SBE-61 CTDs in the southwest Pacific indicate that the sensors are stable in abyssal temperature/salinity characteristics, to ±0.001 PSS-78 for more than a year, at constant potential temperature (Fig. SB3.3). These instruments have not yet achieved the absolute accuracy targets set for them (0.001°C, 0.002 PSS-78, and 3 dbar) but are approaching those standards. Additional validation experiments are planned for SBE-41 and SBE-61 CTDs.

CONT. SIDEBAR 3.2: DEEP ARGO: SAMPLING THE TOTAL OCEAN VOLUME—N. ZILBERMAN

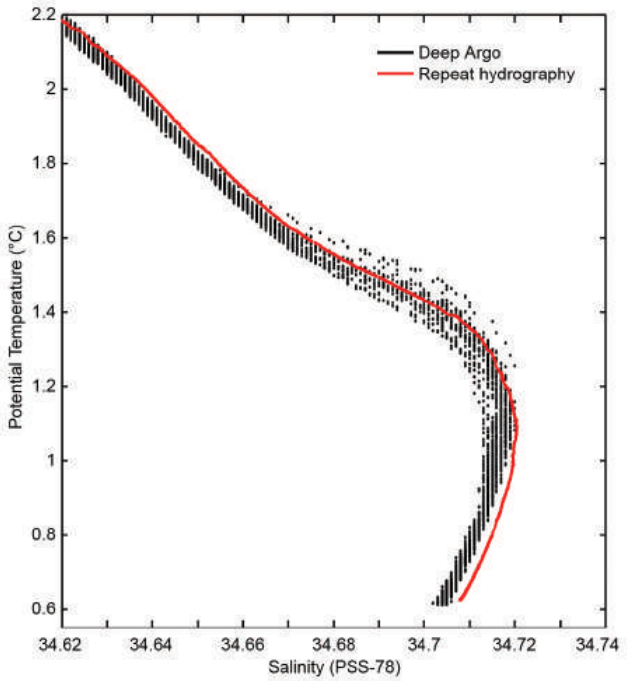

FIG. SB3.3. Temperature/salinity (θ/S) relationship in the southwest Pacific basin. Black symbols indicate 75 Deep SOLO float profiles spread over 30.4°–35.2°S and 172.8°–174.5°W between Feb 2016 and Jan 2017 (www.usgodae.org/ftp/outgoing/argo/dac/aoml/5902447). The red line is a single cast at 35°S from the P15S repeat hydrographic transect of June 2016 (Source: data courtesy of Bernadette Sloyan, CSIRO.)

Several national programs are now deploying regional pilot Deep Argo arrays to demonstrate the feasibility, capabilities, and scientific value of full-depth global ocean observations, and to validate the accuracy of the CTD data against the requirements for abyssal sampling. Results from the pilot arrays are being assessed to revisit the global design of Deep Argo and its objectives. As of February 2017 there were 64 Deep Argo floats either active or registered for deployment in the next few months, including 33 Deep SOLOs, 3 Deep APEXs, 5 Deep NINJAs, and 23 Deep Arvors (Fig. SB3.4). Present Deep Argo pilot arrays are in the North Atlantic, southwest Pacific, Indian, and Southern Oceans. These arrays will be supplemented with additional floats for increasing their areal extent, and an additional pilot array is planned for the Brazil basin in the South Atlantic. The array in the south Australian basin will be extended poleward into the Australian Antarctic basin. Overall, the locations of pilot arrays have been chosen to include regions having stable abyssal temperature–salinity relations and ample hydrographic reference data for CTD validation, regions with previously identified abyssal warming trends, and regions close to water mass formation zones. In the next few years, the expansion of regional pilot arrays will grow toward global implementation of the Deep Argo Program.

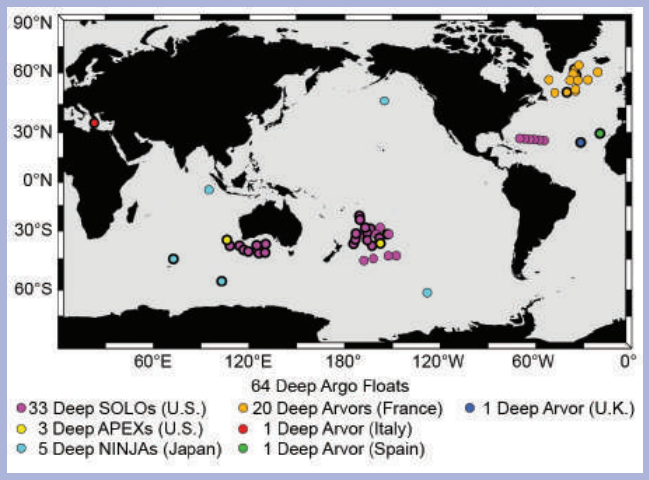

FIG. SB3.4. Location of active Deep Argo floats in Feb 2017 (rounded symbols with thick black contours): 19 Deep SOLOs (U.S.), 3 Deep APEXs (U.S.), 2 Deep NINJAs (Japan), 3 Deep Arvors (France), 1 Deep Arvor (Italy), 1 Deep Arvor (Spain), and 1 Deep Arvor (U.K.). Location of deployments scheduled later in 2017 (rounded symbols with thin black contours) for registered Deep Argo floats: 14 Deep SOLOs (U.S.), 3 Deep NINJAs (Japan), and 17 Deep Arvors (France). (Source: www.jcommops.org.)

2016). This change is likely related to the transition from a strong El Niño in 2015 to a weak La Niña in 2016 and the associated equatorial precipitation (see Fig. 3.12) and wind stress changes (see Fig. 3.13).

Through mid-2016 the Indian Ocean continued to show a similar salinity anomaly structure to that of the previous four years in the upper 300 m, with a fresh surface anomaly from 0 to 75 m and a salty subsurface anomaly from 100 to 300 m (Fig. 3.9e). However, from mid-2016 onward, this salty subsurface anomaly extended from the surface down to ~250 m depth. From 2015 to 2016 salinity increased from 0 to 200 m, with a maximum of about 0.02 at 50 m, while freshening occurred from 250 to 500 m, with a maximum of ~ −0.008 at 300 m (Fig. 3.9f).

Zonally averaged salinity in the upper 75 m of the tropical Atlantic (2°S–22°N) increased by at least 0.06 from 2015 to 2016 (Fig. 3.10a), with a maximum (~0.12) at the surface between 10° and 16°N. This band is primarily responsible for the near-surface positive salinity anomaly during 2016 (Fig. 3.9b). There is notable freshening (< −0.03) from 0 to 50 m centered at 41°N, but it is shifted south and confined to a smaller region than prior years (e.g., 2015 minus 2014, see Reagan et al. 2016). Additionally, there is strong (< −0.06) subsurface freshening from 100 to 225 m in the South Atlantic from 22° to 15°S and weaker freshening (~ −0.03) in the North Atlantic from 21° to 32°N and 55° to 62°N along similar depths, which are the main contributors to the 100–300 m subsurface freshening (Fig. 3.9b).

Zonally averaged salinity changes in the Pacific from 2015 to 2016 (Fig. 3.10b) show strong (< −0.06) freshening north of 60°N from 0 to 110 m and 160 to 250 m in the northern portions of the Bering Sea. Additionally, there is freshening from 0 to 200 m between 39° and 47°N, exceeding −0.12 at 125 m. The tropical Pacific experienced salinification (> 0.03) in the upper 50 m between 3°S and 17°N from 2015 to 2016 and freshening (< −0.03) in both poleward directions from 18° to 27°N (extending and deepening to the south reaching ~250 m at around 8°S) and 12° to 4°S, which is a direct reflection of the transition from a strong 2015/16 El Niño to a weak 2016 La Niña (as discussed in Section 3d2). Farther south, there is a broad region (between 30° and 13°S) of salinification in the upper 100 m, deepening to 150 m around 10°S.

Zonally averaged salinity changes in the Indian Ocean from 2015 to 2016 (Fig. 3.10c) show freshening (< −0.03) between 10° and 15°N in the upper 100 m, with maximum freshening (< −0.09) occurring at the near-surface (0–30 m). This freshening was primarily located in the Bay of Bengal (see Fig. 3.7b) and may be associated with increased river runoff due to a stronger India monsoon in 2016 than in 2015 (see Fig. 7.47). Salinification occurred in the upper 100 m from 16° to 25°N, with a maximum exceeding 0.18 at 50 m and a narrow swath extending to 250 m at 18°N. Between 0° and 8°N and between 18° and 2°S the salinity increased (> 0.03), with the former extending down to ~75 m and the latter to ~100 m. Finally, freshening (< −0.03) occurred between 45° and 40°S in the upper ~125 m. The broad-scale salinification in the upper 200 m of the southern Indian Ocean in conjunction with the large salinification around 18°N were the primary contributors to the near-surface salinification (Fig. 3.9f).

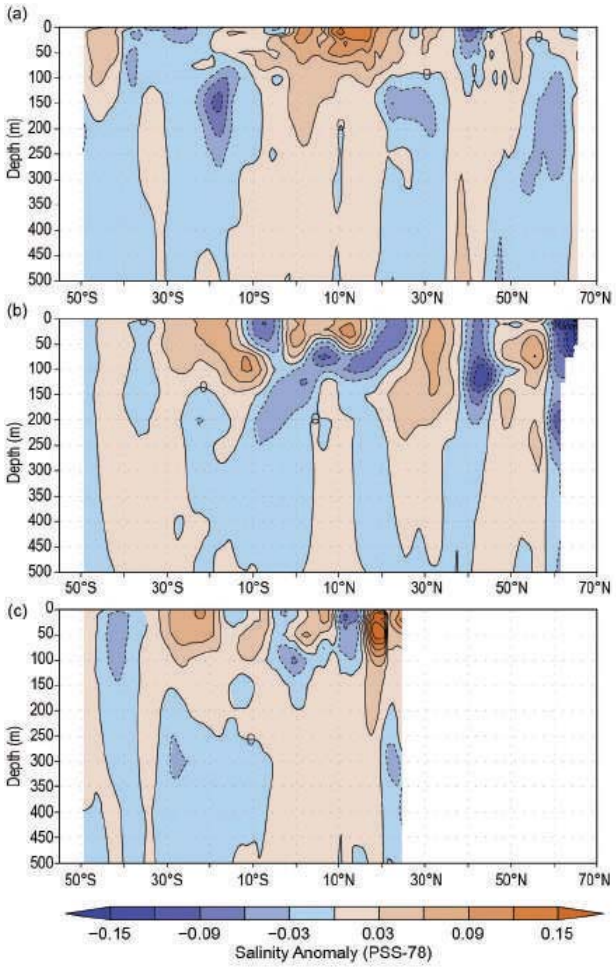

Fig. 3.10. Difference between the 2016 and 2015 zonally averaged monthly salinity anomalies from 0 to 500 m color contoured at 0.03 intervals (black lines, zero contour bold) for the (a) Atlantic, (b) Pacific, and (c) Indian Oceans. Anomalies are relative to the long-term WOA13v2 monthly salinity climatology (Zweng et al. 2013).

e. *Global ocean heat, freshwater, and momentum fluxes*—L. Yu, X. Jin, S. Kato, N. G. Loeb, P. W. Stackhouse, R. A. Weller, and A. C. Wilber

The ocean and the atmosphere communicate physically via interfacial exchanges of heat, freshwater, and momentum. These air–sea fluxes are the primary mechanisms for keeping the global climate system in balance with the incoming insolation at Earth's surface. Most of the shortwave radiation (SW) absorbed by the ocean's surface is vented into the atmosphere by three processes: longwave radiation (LW), turbulent heat loss by evaporation (latent heat flux, or LH) and by conduction (sensible heat flux, or SH). The residual heat is stored in the ocean and transported by the ocean's surface circulation, forced primarily by the momentum transferred to the ocean by wind stress, as well as diffusive processes. Evaporation connects heat and moisture transfers,